

Time-dependent behavior in a transport-barrier model for the quasi-single helicity state

P W Terry and G G Whelan

Department of Physics, University of Wisconsin–Madison, Madison, Wisconsin 53706

Received 13 January 2014, revised 17 March 2014

Accepted for publication 4 April 2014

Published 13 August 2014

Abstract

Time-dependent behavior that follows from a recent theory of the quasi-single-helicity (QSH) state of the reversed field pinch is considered. The theory (Kim and Terry 2012 *Phys. Plasmas* **19** 122304) treats QSH as a core fluctuation structure tied to a tearing mode of the same helicity, and shows that strong magnetic and velocity shears in the structure suppress the nonlinear interaction with other fluctuations. By summing the multiple helicity fluctuation energies over wavenumber, we reduce the theory to a predator–prey model. The suppression of the nonlinear interaction is governed by the single helicity energy, which, for fixed radial structure, controls the magnetic and velocity shearing rates. It is also controlled by plasma current which, in the theory, sets the shearing threshold for suppression. The model shows a limit cycle oscillation in which the system toggles between QSH and multiple helicity states, with the single helicity phase becoming increasingly long-lived relative to the multiple helicity phase as plasma current increases.

Keywords: turbulence, transport barrier, quasi-single helicity

(Some figures may appear in colour only in the online journal)

1. Introduction

In reversed field pinch (RFP) discharges there is normally a spectrum of tearing mode fluctuations resonant on rational surfaces. Innermost resonant modes are unstable; modes resonant at larger radii are driven nonlinearly by mode coupling with the unstable modes, producing a cascade. With each rational surface characterized by its own helicity, this situation is referred to as the multiple helicity state. In recent years a second fluctuation state has been found for operation at higher current [1, 2]. In this situation the innermost resonant tearing mode has an amplitude that significantly exceeds the amplitudes of other helicities, producing a spectrum dominated by a single helicity. Single and multiple helicity states are not stationary. Rather, the system toggles between the two states [3]. At higher current the single helicity phase becomes increasingly long relative to the multiple helicity phase. Comparisons between RFX and MST RFP devices, which operate with different plasma currents, temperatures, and densities, have shown that the transition from a purely multiple helicity state to the dithering quasi-single helicity (QSH) state occurs in both

devices at approximately the same Lundquist number [4]. The time-dependent QSH is thus understood to be a high Lundquist number phenomenon.

Early approaches to understanding the QSH state have tended to view it as a helical equilibrium embedded in an axisymmetric plasma. In simulation the situation is generally found only for low Hartman number, and features a dominant helicity that does not correspond to a core resonant mode [5]. Recent magnetohydrodynamic (MHD) simulations of the transition to this state are reminiscent of the viscous laminarization of hydrodynamic turbulence for decreasing Reynolds number, and are not generally compatible with high Lundquist number conditions [6]. A high Lundquist number QSH state has been observed in MHD simulations, but only by externally forcing the plasma with a helical perturbation at the plasma surface matching the helicity of the QSH [7]. To overcome the limitations of these approaches in providing a realistic description of the QSH state it is becoming increasingly apparent that models that are fundamentally time dependent are needed.

One such model treats QSH not as an equilibrium but as a coherent fluctuation structure that dominates other fluctuations by actively suppressing them through shears in the magnetic and flow fields of the dominant structure [8]. If the dominant fluctuation is the innermost resonant tearing mode, the suppression of other modes also suppresses the mode coupling on which other modes rely for nonlinear drive. This supports the dominance of the innermost resonant mode and quenches modes resonant at larger radii. With the mode coupling suppressed the dominant mode suffers virtually no nonlinear interaction, and hence, nonlinear decorrelation. The innermost mode consequently can become so long lived that it looks like an equilibrium. Under these circumstances the shears of the innermost resonant mode suppress any kind of fluctuation and thereby also establish a transport barrier to heat and particles. Both the magnetic and flow shears of the dominant mode can participate in the suppression of other modes. Stable flow shear is understood to suppress fluctuations driven by other gradients, as it does in the H-mode [9]. Magnetic shear has a comparable effect on magnetic fluctuations, effectively shearing the phase fronts of Alfvénic fluctuations [10]. The model describing the interaction of a dominant mode and secondary fluctuations is intrinsically time dependent. Prior analysis, to describe the physics of the suppression mechanism, assumed situations with steady behavior [8]. This paper extends analysis to time-dependent situations and addresses specific features of the QSH state.

Nonlinear time dependent behavior of transitions between finite-duration quasi stationary states have frequently been described by reduced models sometimes referred to as predator–prey models. Such models have been used to describe the dynamics of the L–H transition [11], internal transport barriers [12], internal heating from cold pulse propagation [13], and other problems. The reduction is designed to remove non essential complexity while retaining the physics that produces gross features of the evolution. The dynamics of such models is more transparent than that of more complete models. If essential features of the transition phenomenon as observed in experiment are reproduced by the reduced model, there is an indication that key processes have been identified. In this paper we build a set of reduced equations for the coupling of a dominant fluctuation and secondary modes model based on the reduced MHD model of Kim and Terry [8]. Analysis of its time-dependent behavior provides a mechanistic description of QSH transitions and an explanation for observed experimental features, the most important being the scaling of the persistence of the QSH phase with respect to plasma current [3].

2. Suppression of mode coupling by magnetic and velocity shear

The tearing mode fluctuation has a mode structure with radial profiles for magnetic field and flow. These have an inner layer at the resonant magnetic surface but extend globally. The magnetic field fluctuation of the innermost resonant tearing mode extends over most of the minor radius, the flow is more localized. If the shear of these profiles is sufficiently large, it can suppress other fluctuations, rendering them stable, reducing

amplitudes and the radial overlap required for interaction, or disrupting the phase required for interaction. Suppression of turbulence or fluctuations by the stable shear of a mean flow or zonal flow is well known [9]. Suppression of one fluctuation by another is also possible by the same mechanism. When it occurs the suppressing fluctuation is no longer subject to turbulent decorrelation and becomes a long-lived coherent structure. Such coherent structures are known to occur in decaying 2D Navier–Stokes turbulence [14]. To suppress ambient fluctuations their shear must exceed a threshold. This requires large amplitude for a given scale size, placing them in the tail of the probability distribution function [15]. Coherent filaments of current and density can also form at the scales of kinetic Alfvén wave turbulence in the interstellar medium and account for scaling features of pulsar scintillation [10]. In that case magnetic shear in one fluctuation suppresses other magnetic fluctuations. The shear threshold for suppression again places the suppressing fluctuation in the tail of the probability distribution function.

In the case of coherent vortices in 2D Navier–Stokes turbulence there is no magnetic field; for kinetic Alfvén waves there is no flow shear. For tearing modes in the RFP, there is both magnetic field and flow. A minimal description for a reduced model should incorporate both shears and the nonlinear interaction between modes. Reduced MHD is attractive because it provides a reasonably simple starting point for a problem that becomes complex because there are two shearing fields and two fluctuating fields. The dimensionless reduced MHD equations apply under the assumption of $\mathbf{B}_0(x) = B_z \hat{z}$, and are given by

$$\frac{d\omega}{dt} + \nabla_{\parallel} j = 0, \quad (1a)$$

$$\frac{d\psi}{dt} + \nabla_{\parallel} \phi = 0. \quad (1b)$$

Here $\omega = \nabla_{\perp}^2 \phi$ is the vorticity, $j = \nabla_{\perp}^2 \psi$ is the current (defined in the opposite direction of the true current), and the parallel and total derivatives are

$$\nabla_{\parallel} f = \hat{\mathbf{b}}_0 \cdot \nabla f - [\psi, f] = \frac{\partial f}{\partial z} - [\psi, f],$$

$$\frac{df}{dt} = \frac{\partial f}{\partial t} + [\phi, f],$$

$$\text{where } [f, g] = \frac{1}{r} \left(\frac{\partial f}{\partial r} \frac{\partial g}{\partial \theta} - \frac{\partial g}{\partial r} \frac{\partial f}{\partial \theta} \right).$$

For cylindrical geometry with the periodicity in the azimuthal and axial directions, a Fourier expansion gives

$$f(r, \theta, z, t) = \sum_{m,k} f_{mk}(r, t) \exp i(m\theta - kz).$$

The theory for suppression of secondary magnetic modes by a dominant mode used reduced MHD [8]. It utilized a two-time scale analysis to separate secondary modes from the primary mode. The former evolve on a fast time scale in the presence of the slowly varying shears of the primary mode. The latter evolve on the slow scale under the average interaction with rapidly varying secondary modes. Under the two-time scale expansion, shearing is expressed as a rate associated with

the radial derivative of the poloidal flow and magnetic field fluctuations of the dominant mode. These rates are given by

$$\Omega'_\phi = \frac{im}{r} \frac{\partial \phi}{\partial r} \Big|_{n=6}, \quad (2)$$

$$\Omega'_\psi = \frac{im}{r} \frac{\partial \psi}{\partial r} \Big|_{n=6}, \quad (3)$$

where $|_{n=6}$ is a label intended to identify the dominant mode, which for concreteness we take to be $n = 6$. These two shearing rates combine to form a composite shearing rate. The combination is complex, but if one shear dominates the other it can be taken to be

$$\Omega' = \frac{im}{r} \text{Max} \left[\frac{\partial \phi}{\partial r} \Big|_{n=6}, \frac{\partial \psi}{\partial r} \Big|_{n=6} \right]. \quad (4)$$

Equation (4) indicates that, in terms of the effect of a dominant mode on other fluctuations, a single calculation can be carried out that treats either the effect of flow shear or magnetic shear, provided one is larger than the other. We pursue this course for its generality, noting that the results derived below will hold in either case.

It is nevertheless of interest to know which effect is stronger. It is known that for shear flow to affect a tearing mode it must satisfy

$$\frac{v}{L_\phi} \geq \frac{V_A}{a}, \quad (5)$$

where v is the flow speed, V_A is the Alfvén velocity, a is the minor radius and L_ϕ is the scale length of the shear [16]. While the shear scale length of the fluctuating flow of the dominant mode is smaller than that of the fluctuating magnetic field in linear theory, the flow itself is also smaller than V_A . Estimates of these quantities from experimental measurements suggest the two terms in the inequality (5) could possibly be comparable, but do not provide sufficient resolution for a firm determination. As this is a matter of further experimental measurement, it is outside the scope of the present theoretical effort.

When the shearing rate is larger than the nonlinear decorrelation rate, overlapping fluctuations experience a boundary layer. In the boundary layer, fluctuation amplitudes are curtailed exponentially. The scale of exponentiation is the layer width Δr . It is governed by a balance of the shearing rate Ω' and the nonlinear decorrelation rate. When shear is strong the layer width decreases to maintain the balance. The layer width, which scales like the reduced radial correlation length of fluctuations in H-mode shear layers, is proportional to the inverse square root of the shearing rate,

$$\Delta r = \left(\frac{\phi}{r\Omega'} \right)^{1/2}. \quad (6)$$

The shear of the dominant tearing mode extends globally and suppresses coupled modes whose outer (ideal) region overlaps with the shear. (Note that inner layers do not have to

overlap.) It should also be noted that the shear has a separate effect on the cross phase of interacting fluctuations, and strongly suppresses the correlation required for mode interaction. This latter effect is typically stronger than the exponential curtailment of amplitudes [17]. However, since most secondary modes rely on interaction with the dominant mode for excitation to finite amplitude, it has the effect of strongly reducing secondary mode level.

The effect of shear is weak unless it exceeds a critical value. When shear is quantified by its shearing rate the critical value is the nominal turbulent decorrelation rate. When shear is quantified by its radial layer width Δr the critical value is a radial fluctuation scale. For tearing modes this is the magnetic island width

$$w_0 = \sqrt{rq\tilde{B}_r/mq'B_\theta^{\text{eq}}}, \quad (7)$$

where \tilde{B}_r is the amplitude of the tearing mode and q is the safety factor. If the QSH state is caused by shear suppression, it requires

$$\frac{\Delta r}{w_0} < 1. \quad (8)$$

Because QSH is triggered somewhere near $\Delta r/w_0 = 1$, its persistence acquires a dependence on the equilibrium poloidal field B_θ^{eq} , or plasma current. This dependence is derived in the next section.

3. A reduced model for the nonlinear coupling

We derive a predator-prey model from equations (1a) and (1b), including in each equation the composite shearing rate, equation (4), and a minimal representation of each nonlinearity, yielding

$$\gamma \hat{w}_m + a\Omega' \hat{w}_m = \sum_{m'} \frac{im'}{r} \frac{\partial \hat{\psi}_{m'}}{\partial r} \hat{f}_{m-m'}, \quad (9)$$

$$\gamma \hat{\psi}_m + a\Omega' \hat{\psi}_m = \sum_{m'} \frac{im'}{r} \frac{\partial \hat{\psi}_{m'}}{\partial r} \hat{\phi}_{m-m'}, \quad (10)$$

where for shorthand, the mode numbers m and m' represent spatial mode number pairs (m, n) and (m', n') , and imaginary Fourier frequencies γ and γ' . The sum over m' is understood to include an integral over γ' ; the symbol $\hat{}$ signifies a Fourier transformed quantity. The radial variable is dimensionally represented by the minor radius a . Evaluating equation (9) at wavenumber $m - m'$ and inverting,

$$\hat{\phi}_{m-m'} = \sum_{m''} \frac{(im''/r)(\partial \hat{\psi}_{m''}/\partial r) \hat{\psi}_{m-m'-m''}}{\gamma - \gamma' + a\Omega'}. \quad (11)$$

This result is substituted into equation (10) and the standard wavenumber selection of statistical closure theory from the sum over m'' is used. The result yields

$$\gamma \hat{\psi}_m + a\Omega' \hat{\psi}_m = \sum_{m'} \frac{(-m'^2/r^2)(\partial \hat{\psi}_{m'}/\partial r)^2 \hat{\psi}_m}{\gamma - \gamma' + a\Omega'}. \quad (12)$$

We modify this expression to describe the evolution of the energy-like quantity $|\psi_m|^2$ by multiplying equation (12) by ψ_{-m} and adding it to the complex conjugate of equation (12) multiplied by ψ_m . The right hand side of equation (12) represents a turbulent diffusivity. The finite lifetime of fluctuation correlations that contribute to the diffusivity is represented by the time scale $[\gamma - \gamma' + a\Omega']^{-1}$. Because the phase averaged energy $|\psi_m|^2$ evolves on a slower time scale than the fluctuations that contribute to the diffusivity, the integral over γ' can be subjected to the standard Markovian approximation of closure theory ($\gamma \rightarrow 0$). The result yields

$$\frac{\partial |\hat{\psi}_m|^2}{\partial t} = \sum_{m'} \frac{(-m'^2/r^2)|(\partial \hat{\psi}_{m'}/\partial r)|^2 |\hat{\psi}_m|^2}{\gamma' + a\Omega'}, \quad (13)$$

where we now write $|\hat{\psi}_m|^2$ in the time domain. In reaching this result we have assumed that Ω' is imaginary, in keeping with the conservative character of nonlinearity in MHD. This assumption is consistent with equations (2) and (3) with $\partial\phi/\partial r|_{n=6}$ and $\partial\psi/\partial r|_{n=6}$ respectively as binormal components of a real flow and magnetic field for the $n = 6$ mode. As is standard for energy evolution expressions, the suppressive effect of shear now resides exclusively in the propagator, which forms the denominator of the nonlinear term. When shear becomes large it reduces the nonlinear strength, suppressing the coupling of large scale unstable modes to smaller scale modes. The necessary step of ensuring that the propagator capture the threshold for shear suppression will be undertaken shortly.

Mode coupling resides in the nonlinearity. When $n = 6$ or $n' = 6$ the fluctuation $|\psi|^2$ corresponds to the dominant mode. When n or n' are greater than 6, $|\psi|^2$ corresponds to a secondary mode. We will truncate the sum over n' so that there is a single field $D = |\psi_{n=6}|^2$ for the dominant mode and a single field $S = |\psi_{n>6}|^2$ for the secondary modes. The mode coupling is represented by products of S and D . We consider the following equations for S and D , representing particular mode coupling combinations,

$$\frac{\partial D}{\partial t} = Q_D - \frac{(\sigma_1 S^2 + \sigma_2 SD)}{\gamma' + a\Omega'} - \alpha_D D, \quad (14)$$

$$\frac{\partial S}{\partial t} = Q_S + \frac{(\sigma_2' DS + \sigma_1' D^2)}{\gamma' + a\Omega'} - \beta S^2 - \alpha_S S. \quad (15)$$

The four mode coupling combinations represented by σ_1 , σ_2 , σ_1' and σ_2' occur in statistical closures as couplings between a larger and smaller scale fluctuations. The couplings with σ_2 and σ_2' are referred to as coherent and encompass physical processes such as eddy damping and eddy diffusion that depend on eddy amplitude; those with σ_1 and σ_1' are incoherent, i.e., independent of eddy amplitude. The signs of the coupling terms produce energy transfer from the dominant mode to secondary modes, in accordance with the tearing mode cascade. In addition to the mode coupling, there are external drives Q_D and Q_S , representing the Ohmic free energy. These drives couple to the equilibrium at the largest scales, and are represented by external forces. Since the dominant mode is the primary recipient of the magnetic free energy associated with

the Ohmic drive, $Q_D > Q_S$. The terms with α_D and α_S represent resistive dissipation. Because the dominant mode is larger scale than the secondary modes, $\alpha_D < \alpha_S$. With wavenumber space projected out of this simple representation, dissipation at small scale and Ohmic drive must be distinguished. We give the former its proper amplitude-dependent form, and make the latter an external, amplitude-independent drive. Otherwise the two processes would be lumped together into a single coefficient. A zero value for this coefficient, consistent with a steady state, would be indistinguishable from removing these effects altogether from the model. A positive (negative) value would be indistinguishable from a weak drive with no damping (weak damping with no drive). The term $\beta|S|^2$ represents mode coupling from larger scale secondary modes to smaller scale secondary modes, i.e., the forward energy cascade. This term is present only if S represents a subset of the most prominent secondary modes, in which case it acts as subgrid scale damping. If it represents all secondary modes, this term would be absent. Including or dropping this term does not have a large effect on the time dependent behavior of the model.

The suppression term only becomes important when equation (8) is satisfied. To make the threshold explicit we start with equation (4), assuming $\partial\psi/\partial r > \partial\phi/\partial r$, $m = 1$, and $r \approx a$. Then

$$a\Omega' = \frac{d\tilde{B}_{n=6}}{dr} = \frac{\tilde{B}_{n=6}}{l_B} = \frac{W_0^2 q' B_\theta^{\text{eq}}}{l_B r q} = \frac{W_0^2}{\Delta r^2} \frac{\Delta r^2 q' B_\theta^{\text{eq}}}{l_B r q}, \quad (16)$$

where we have expressed the amplitude of the dominant mode in terms of its island width using equation (7). When the shear-suppression threshold is exceeded, $W_0^2/\Delta r^2 = (D/D_0)^{1/2} > 1$, where D_0 is the dominant mode amplitude squared at the suppression threshold. Therefore the shearing factor can be written

$$\gamma + a\Omega' = 1 + \left(\frac{D}{D_0}\right)^{1/2} \left(\frac{B_\theta^{\text{eq}}}{B_{\theta_0}}\right) \left(\frac{\Delta r}{l_B}\right)^2 \left(\frac{l_B}{a}\right) \left(\frac{a^2 q'}{r q}\right), \quad (17)$$

where B_{θ_0} is the threshold value for the equilibrium poloidal field (or equivalently, plasma current) at which the QSH state first appears. With all quantities referenced to threshold values, the appropriate offset for the shearing factor is 1, as expressed in equation (17). For compactness, we write

$$\gamma + a\Omega' = 1 + \epsilon \left(\frac{D}{D_0}\right)^{1/2}. \quad (18)$$

The quantity $\epsilon = B_\theta^{\text{eq}}(\Delta r)^2 a q' / B_{\theta_0} l_B r q$ is small because while $B_\theta^{\text{eq}}/B_{\theta_0}$ might be somewhat larger than unity for present day RFPs, $a^2 q' / r q$ is order unity, and $(\Delta r/l_B)^2 (l_B/a)$ is quite small. With ϵ small, the ratio of D to its nominal threshold D_0 is large. Since $\epsilon(D/D_0)^{1/2}$ is the suppression factor, we see that suppression is favored by large B_θ^{eq} .

With this result we write the predator-prey model as

$$\frac{\partial D}{\partial t} = Q_D - \frac{(\sigma_1 S^2 + \sigma_2 SD)}{1 + \epsilon(D/D_0)^{1/2}} - \alpha_D D, \quad (19)$$

$$\frac{\partial S}{\partial t} = Q_S + \frac{(\sigma_2' DS + \sigma_1' D^2)}{1 + \epsilon(D/D_0)^{1/2}} - \beta S^2 - \alpha_S S. \quad (20)$$

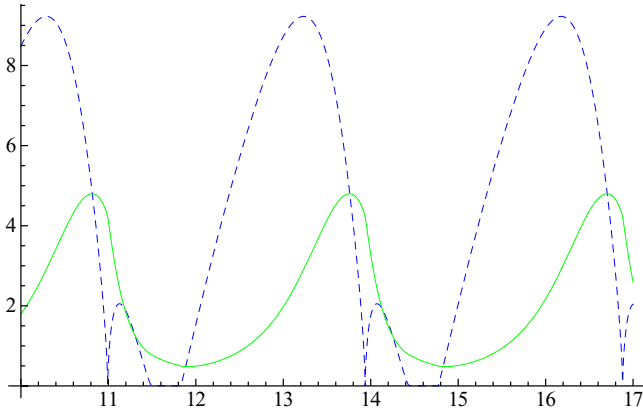


Figure 1. Temporal behavior of a limit-cycle state showing a QSH state that intermittently returns to a multiple helicity state. The blue trace is $|D|$ and the green trace is S .

Although this model is derived from MHD, it has significant limitations. While it is designed to capture temporal dynamics associated with the competition between nonlinear energy transfer and suppression by shear, in other matters it is not realistic. For example, energy is not conserved, including by the nonlinearity. Consequently no absolute scale can be attached to the amplitude D and S , nor is it guaranteed that their values are always positive. Improving the realism of the model and its relation to experiment will require treatment of $m = 0$ modes. This qualitative change in approach is outside the scope of the present study but will be considered in the future.

4. Time-dependent behavior

We consider solutions of equations (19) and (20). Consistent with these types of models, different parameter values lead to solutions with fixed points or limit cycles. For example, if $\sigma_1 = \sigma_2' = 0$ there are decaying relaxation oscillations en route to a fixed point solution. For $\sigma_2 = \sigma_1' = 0$ there is a limit cycle. The limit cycle is sensitive to the value of ϵ in a way that is consistent with suppression, as shown below. Changing values of drive, resistive dissipation and β does not tend to introduce qualitative changes, provided the drive is sufficient to maintain the limit in the presence of dissipative losses.

Figure 1 shows a limit cycle solution with $\sigma_2 = \sigma_1' = 0$. The time traces are typical of predator–prey dynamics. A prey field (blue) is depleted by feeding the predator (green). The predator crashes once its source is depleted, allowing the prey to reemerge under its external drive and the weakened predator. The cycle repeats. The secondary modes (green) are smaller in amplitude because their dissipation is stronger and their external drive is weaker. The rise of D is more gradual than its depletion because the former is linear while the latter is nonlinear. When $D \gg S$, e.g., between $t = 12.2$ and $t = 13.4$, the system is in the QSH state. Otherwise it is in the multiple helicity state.

Suppression by shear is active throughout the limit cycle, but not in a conspicuous way. It is not directly involved in triggers that initiate the depletion of D , or its subsequent recovery. Rather, when it is strong enough to have an effect,

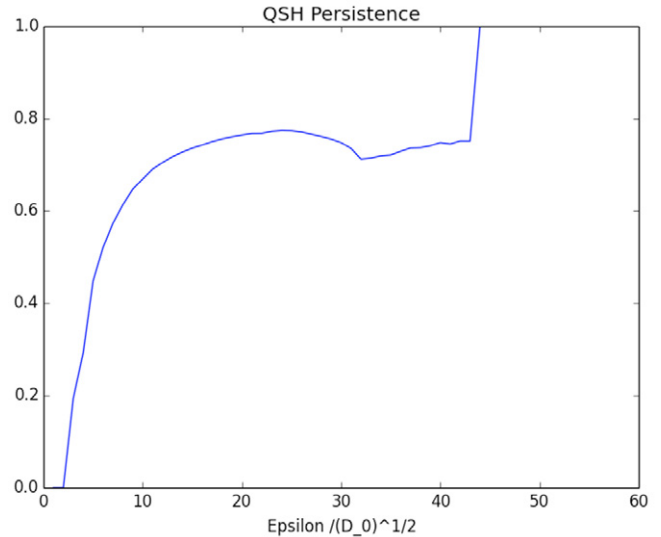


Figure 2. Percent of time the system is in the QSH state with $D \gg S$ as a function of the shearing coefficient ϵ . At 0% and 100% the system transitions to fixed point behavior.

its suppression of the nonlinear interaction simply allows D to survive longer before succumbing to S . To see the role of suppression we must vary $\epsilon/D_0^{1/2}$ and measure the length of the QSH phase. Physically, this variation could be achieved by varying B_θ^{eq} , or equivalently, by varying the plasma current, and observing the percent of time in the QSH phase relative to the multiple helicity phase. The results of this variation are shown in figure 2. It is observed that the QSH time percentage varies from 0 to 100 as the suppression coefficient is increased. The corresponding variation of $\epsilon/D_0^{1/2}$ from order unity to ~ 40 represents the suppression strength required to go from no effect on the predator–prey cycle to complete elimination of the cycle by inhibiting the interaction. This plot, which is the central result of this paper, demonstrates that the composite shearing effect of equation (4) is capable of moderating limit cycle behavior between QSH and multiple helicity states, and that it evinces a scaling with plasma current or poloidal field that is consistent with experiment.

The endpoints of the QSH percent time variation represent transitions from limit cycle behavior to fixed point behavior. At the 100% level, the system locks into a state in which the amplitudes of D and S are steady with $D \gg S$. A time history plot for this type of behavior is shown in figure 3. Even though the system is permanently in the QSH state, nonlinear transfer from the dominant mode to secondary modes is not zero, as indicated by the finite level of S . If ϵ is further increased, the amplitude of S becomes smaller until it reaches zero. This state is a resistive single helicity state with negligible nonlinear activity. Its appearance here is enabled by the form of the nonlinear transfer, which itself vanishes as $S \rightarrow 0$. The nonlinear transfer of a parametric instability process, wherein two wavenumbers of a large amplitude mode pump small amplitude modes could maintain the QSH limit cycle. However, if there is a single mode number $n = 6$ for the dominant mode, the parametric process is not possible.

When the QSH percent time is zero the system is in a state with $S > D$. A time history for this situation is given in

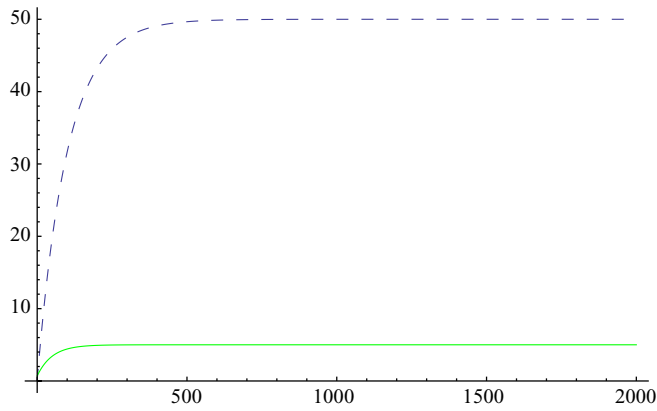


Figure 3. Time history of the system for the fixed point that occurs when the QSH persistence reaches 100%. The blue trace is D and the green trace is S .

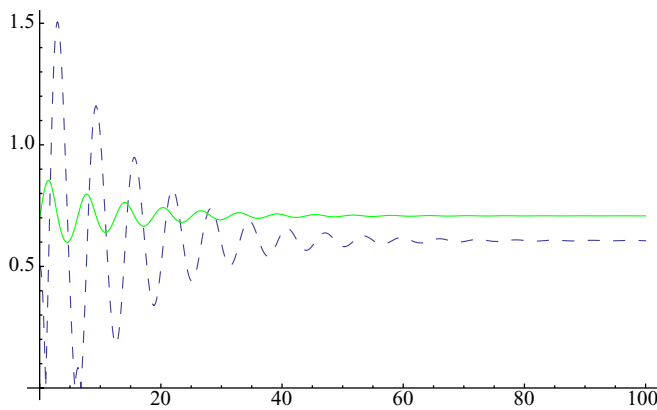


Figure 4. Time history of the system for the fixed point that occurs when the QSH persistence reaches 0%. The blue trace is D and the green trace is S .

figure 4. There is a very slow relaxation oscillation towards an asymptotic steady state with S slightly larger than D .

The nonlinear coupling explored in figures 1–4 couples fluctuations of different scales in ways that are generally consistent with MHD. However, any exercise in a more direct matching of model couplings to experiment immediately reveals shortcomings that should be addressed. For example, including $m \neq 1$ modes (e.g., $m = 0$), which are necessary to couple toroidal modes with $m = 1$, would capture an important aspect of mode coupling as it is understood from experiment and allow a realistic description of energy conservation. This approach, which enlarges the model to three fields, will be explored in future work.

5. Analysis

It is possible to determine the effects that dominate at various times during the evolution of the limit cycle shown in figure 1 by examining the magnitude of the terms in equations (19) and (20). These times correspond to three transition points and two time ranges. The points are the times when S transitions from growth to decay and D comes into parity with S , when D begins a phase of steep rise, and when the rise of D saturates. The time ranges correspond to the decay of D and growth of S ,

and the steep rise of D . This analysis essentially explains the interaction of the various terms in the model and informs the question of whether modifications of its makeup are desirable to better replicate behavior observed in experiment. While modifications could improve the model, this analysis supports the conclusion that the effect of shear, drive and dissipation, and nonlinear transfer between fluctuations, support a limit cycle oscillation with growing QSH persistence as B_θ^{eq} rises.

We consider first the time range in which S is growing and D is large. The growth of S is caused primarily by nonlinear transfer between the dominant and secondary modes. This transfer slows the growth of D before its maximum near $t = 13$, and then causes a rapid decay. Because of resistive losses and transfer to high n in the S equation, the growth of S is not as fast as the loss of D . However, because S is growing, nonlinear transfer and the small drive Q_S are larger than the dissipative terms representing transfer to high n and resistive decay.

At a critical time just before $t = 13.8$, D drops below a level necessary for the nonlinear transfer into S to overcome transfer to high n and resistive damping. From equation (20) the nonlinear transfer is given by $\sigma_2' DS/[1 + \epsilon(D/D_0)^{1/2}]$. The transition is triggered by the relative smallness of D in the numerator. At this transition time S abruptly changes from growth to decay. Shearing is not a key effect here—the system is in a multiple helicity phase.

At a second critical time before $t = 14.8$, D initiates a sharp rise triggered by the smallness of S , which in turn reduces nonlinear transfer out of D . The nonlinear transfer rate from D , which equation (19) gives as $-\sigma_1 S^2/[1 + \epsilon(D/D_0)^{1/2}]$ drops below a level for which it can balance the Ohmic drive, initiating the rise. This effect is governed by the factor $S^{1/2}$ in the denominator of the transfer rate. At the transition, shear is not a player, because the level of D is similar to its level at $t = 13.8$, where the system is in a multiple helicity state. However, the rise of D is sufficiently rapid that shear suppression quickly comes into play. Around $t = 15$, S begins to grow because the nonlinear transfer rate into S is rapidly rising with D , and transfer to high n , which goes like βS^2 , is weaker for S small. The growth remains slow even as D becomes large because shearing comes into play and limits the transfer rate.

The steep rise of D saturates and begins a slow decline at a third critical time around $t = 16.1$. This transition occurs because the Ohmic drive is independent of D while the resistive decay $\alpha_D D$ is proportional to D . At a critical value of D resistive decay overcomes the drive. Nonlinear transfer also helps saturate the growth of D , but the transfer is significantly slowed by shearing.

From the above analysis we conclude that shearing is not a player in the sudden transitions of this model. Its role is to set the duration of the time range in which D is large, which constitutes the QSH state. This analysis fully supports the behavior of figure 2, which shows that QSH persistence is proportional to the strength of shearing. The transition triggers are sensitive to the form of the nonlinearities, and could change if other forms for the coupling are used. However, all nonlinearities involving the coupling between the dominant and secondary helicities will involve a suppression factor, and its form will

be that given by equation (18). Therefore, because suppression is strong when D is large, the persistence of QSH with shearing strength will not be altered by changes in the form of nonlinear coupling. Consequently, the effect of shear on the establishment of QSH, which was demonstrated in [8], and its effect on the duration of limit cycle oscillations between QSH and multiple helicity states, are robust aspects of the theory.

6. Conclusions

While early theoretical and numerical work has fostered a tendency to view the QSH state as a helical equilibrium, experimental observations of dithering between QSH and multiple helicity states, and the tendency of high current operation to favor QSH, have undermined the credibility of an equilibrium paradigm. In this paper we have shown that both of these key experimental observations follow naturally from a picture of QSH in which the coupling between the innermost resonant tearing mode and secondary tearing modes, which strongly rely on nonlinear transfer for excitation, is suppressed by the shears of magnetic field and flow of the innermost mode. That shears of magnetic field and flow associated with one fluctuation structure can suppress coupling with other fluctuations has been established previously. Here we have shown that this effect is fully compatible with limit cycle behavior that toggles between states where the innermost mode strongly dominates all others by virtue of shear suppression and ones where all modes interact, with shearing too weak to suppress the interaction. Importantly, the suppression model shows that large equilibrium poloidal field is conducive to a stronger shearing effect, and that this behavior leads to stronger QSH persistence as the equilibrium field is increased through stronger Ohmic drive.

These conclusions have been established through a time-dependent model based on reduced MHD. In this model the dominant and secondary modes are described by single fields in a set of predator–prey equations. The triggers for the transitions that occur between QSH and multiple helicity phases

are set by the nonlinear coupling. However, the duration of the QSH phase is governed by the strength of shearing. The form of the suppression factor is derived from standard statistical closure theory. It enters as a linear shearing rate in the turbulent decorrelation time and is consequently independent of the form of the nonlinear coupling. The general conclusions drawn from the model thus transcend its least robust details and support the notion that the QSH state represents a suppression of nonlinear energy exchanges between dominant and secondary modes by magnetic and flow shear.

Acknowledgments

The authors acknowledge useful conversations with Vladimir Mirnov, Juhung Kim and Andrew Ware. This work was supported by US Department of Energy Grant DE-FG02-85ER53212.

References

- [1] Martin P *et al* 2003 *Nucl. Fusion* **43** 1855
- [2] Bergerson W F *et al* 2011 *Phys. Rev. Lett.* **107** 255001
- [3] Lorenzini R *et al* 2009 *Nature Phys.* **5** 570
- [4] Chapman B *et al* *Phys. Plasmas* submitted
- [5] Cappello S and Escande D F 2000 *Phys. Rev. Lett.* **85** 3838
- [6] Schnack D D 2013 private communication
- [7] Bonfiglio D, Veranda M, Capello S, Escande D F and Chacón L 2013 *Phys. Rev. Lett.* **111** 085002
- [8] Kim J-H and Terry P W 2012 *Phys. Plasmas* **19** 122304
- [9] Terry P W 2000 *Rev. Mod. Phys.* **72** 109
- [10] Terry P W and Smith K W 2008 *Astrophys. J.* **665** 402
- [11] Diamond P H, Liang Y-M, Carreras B A and Terry P W 1994 *Phys. Rev. Lett.* **72** 2565
- [12] Diamond P H *et al* 1997 *Phys. Rev. Lett.* **78** 1472
- [13] Diamond P H, Lebedev V B, Newman D E and Carreras B A 1995 *Phys. Plasmas* **2** 3685
- [14] McWilliams J 1994 *J. Fluid Mech.* **146** 21
- [15] Terry P W, Newman D E and Mattor N 1992 *Phys. Fluids A* **4** 927
- [16] Gatto R, Terry P W and Hegna C C 2002 *Nucl. Fusion* **42** 496
- [17] Terry P W, Newman D E and Ware A S 2001 *Phys. Rev. Lett.* **87** 185001